Cold spray metal coating of wood for cabinet making applications

Patrizio LOMONACO, Antoine DEBRAY, Francesco DELLORO, Michel JEANDIN
MINES ParisTech, MAT-Centre des Matériaux, 91003, Evry, France
patrizio.lomonaco@mines-paristech.fr
Bernardo FAVINI
Facoltà di Ingegneria Civile ed Industriale, University of Rome Sapienza, via Eudossiana 18, 00189 – Rome, Italy
Arnaud BOUSQUET
Matériaupôle,6 Rue Pasteur, 94400 Vitry-sur-Seine
Steven LEPRIZE'
ARCA ébénisterie,12-14 Rue Graham Bell, 77600 Bussy-Saint-Georges

Abstract

Thermal spray technology has been widely used in the last decades for creating coatings onto metal substrates. This study is focused on an original metal-wood assembly obtained by cold spray. A constant correlation between experimental and numerical tests has been adopted to assess and improve the possibilities of this coupling. First, the analysis of geometrical features of the wood structure at the microscale was necessary to identify the properties of the deposition surface. Next, a wide range of cold spray tests was conducted to obtain metal coatings onto four species of wood. To better understand the dependency of deposition efficiency for the process from particle state conditions, a computational fluid-dynamics tool is in development to compute particle speed and temperature. Then, a series of finite element simulations of single and multi-particle impacts onto local structures of the wood, as observed from SEM and microtomography images of the specimens. A classical pull-off test of the specimen has been used to collect data about adhesion strength and behavior. A numerical counterpart of the test has been developed. Enabling the comparison of macroscopic adhesion behaviour of the real interfaces with that of virtual interfaces.

Introduction

Thermal spraying techniques are additive processes in which melted or solid materials are sprayed onto a surface. Cold spray(CS) is part of this family. In this process, particles are accelerated in a de Laval nozzle towards a substrate by a heated high pressure gas. The main difference with other thermal spraying techniques is that particles maintain their solid state. This technology is industrially assessed only for metal powders and substrates. Recent studies begun to involve other kinds of substrates. The intent of this study is to extend CS to novel dissimilar material couples, in particular metal and polymer coatings onto wooden substrates, opening the way to the achievement of multi-material assemblies using no glue. The scientific objective of this work is to understand the mechanisms underlying the coating build-up onto wooden substrates. Because of the fibrous, brittle and thermosensitive features of the substrate, impact conditions must be optimized and phenomena at micro and macro scale should be analyzed to understand particle anchoring and coating building process. This modeling approach, going from the micro to the macro scale, is the only one being able to address effectively the problem of cold spray deposition onto a complex material, like the wood proposed in this study

Materials and methods

Substrate

Four different types of wood have been studied, all from the family of hardwoods: walnut, sycamore, ash and oak. Arca (Bussy-Saint-Georges, France) cabinet maker provided wooden plates, as an industrial partner involved in this project.

The particularity of hardwood is the presence of structures called vessels (absent in softwoods), dedicated only to the transport of sap and water and without a structural function. To better understand the morphological structure of the specimens a full characterization of the material has been done, by means of SEM and optical microscopy.

Due to its orthotropic characteristics, three main sections (planes) are generally identified in wood: transversal, radial and tangential, as shown in Fig. 1.

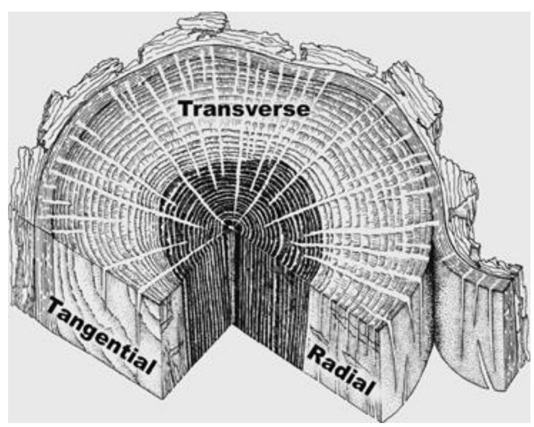

Fig.1 : Wood main planes from [1]

The repeating units forming the structure, as shown in Fig. 2, are called fibers and have sizes in the order of 5-40 µm. Vessels are larger pores (100-200 µm), delimited by cell walls. Rays are made of cells of a different kind and can be considered as inclusions of another material. These features are different for every wood species. Here, only sycamore was chosen to be presented, due to its better performance in terms of deposition efficiency.

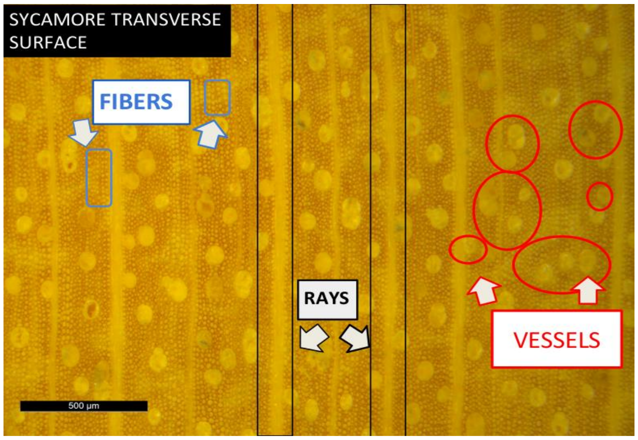

Fig.2: optical images of the transverse surface of sycamore showing the main features of wood.

For the cold spray experiments, cubic specimens of dimension 1 cm^3 were used as the substrates. Prior to cold spraying, substrates were polished with SiC grinding paper (up to grit size 1200) and ethanol as lubricant.

Powders

The powders used in this work were commercial-purity aluminium (irregular shape), tin (irregular shape), copper (spherical shape), PEEK (irregular shape), zinc (spherical shape), with average particle sizes of 45, 63, 65, 17 and 20 µm, respectively.

The scanning electron microscope images are shown in Fig. 3.

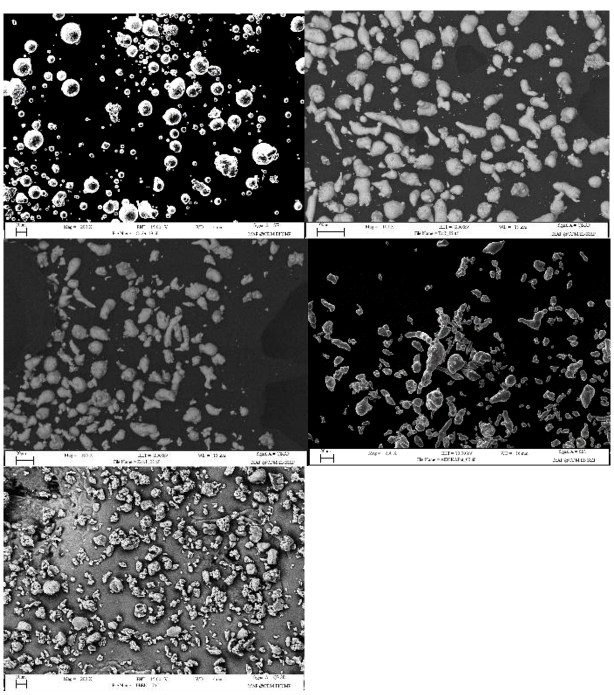

Fig.3 : SEM top views of sprayed powders, left column from the top copper. zinc and PEEK powders; right column from the top tin and aluminium powder.

Cold spray equipment

Both high pressure (HPCS) and low-pressure (LPCS) cold spray equipment were used.

The HPCS was a CGT Kinetics 3000 Cold Gas Technology-GmbH, Germany, used with nitrogen as the principal gas. Spraying parameters used for aluminium and tin powders are presented in Table1.

The LPCS system was a Dymet 523 from Dycomet (Akkrum, The Netherlands), used for spraying aluminum, copper, zinc, tin and PEEK powders with compressed air as principal gas and spraying parameters are presented in Table 2.. With respect to the high pressure systems, LPCS provided a downstream injection of the particles (*i.e.* after the nozzle throat), decreasing the risk of clogging inside the throat. Nitrogen was also used as carrier gas for the LPCS work.

Table 1: high pressure cold spray parameters

Powder	Gas Temperature °C	Gas Pressure (MPa)	Stand-off distance (mm)	Transverse Speed (mm/s)
Aluminium	100 to 350	1 to 2.5	10 to 40	100 to 300
Tin	50 to 270	0.8 to 1.1	20 to 80	100

Table 2: low pressure cold spray parameters

Powder	Gas Temperature °C	Gas Pressure (MPa)	Stand-off distance (mm)	Transverse Speed (mm/s)
Aluminum	400 to 600	0.4 to 0.6	20 to 40	100 to 200
Tin	300 to 450	0.4 to 0.6	20 to 40	100 to 200
Copper	350 to 600	0.4 to 0.6	20 to 40	100 to 200
Copper/Zinc	400-500	0.4 to 0.6	20 to 40	100 to 200
Zinc	400-500	0.4 to 0.6	20 to 40	100 to 200
Copper/Peek	300-500	0.4 to 0.6	20 to 40	100 to 200

Specimens were characterizer with a ZEISS DSM982 Gemini SEM and a LEICA DMI 5000 optical microscope equipped with a camera.

Results

High pressure cold spray

No successful deposition was obtained with aluminum powders for any of the parameters tested. Erosion of the wooden substrates proved to be the limiting factor that prevented obtaining a coating. Sprayed aluminum particles eroded the wood structure, probably hitting the fiber surface too hard. In these conditions, fiber damage would absorb kinetic energy from the particles, preventing sufficient deformation of the latter. In the SEM top view shown in Fig. 4, one can note groups of particles stacking in some regions, while in other regions only eroded wood areas are visible.

The lack of particle plastic deformation, which is essential for the formation of the coating, clarifies why the standard mechanisms of coating build up did not operate there. Nevertheless, these first tests showed that the transversal section and sycamore wood species had a better behaviour in terms of resistance to erosion. It was then decided to use only transverse samples for the remaining testing, thus leaving radial and tangential surfaces for future work.

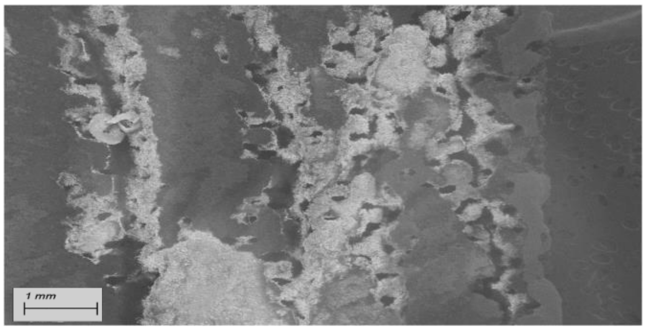

Fig.4:Top view of the eroded transverse surface

Further cold spray tests were performed with tin powder, with the purpose of avoiding strong erosion and to tin is more easily deformed and deposited than aluminum. This choice of material orientation, powder and parameters led to the first success in obtaining a metal coating onto wood. In fact, despite some traces of erosion, a homogeneous and continuous tin coating was successfully sprayed onto sycamore substrates. The higher the temperature of the gas the higher the thickness of the coating. An SEM image of the coating cross section is shown in Fig. 5.

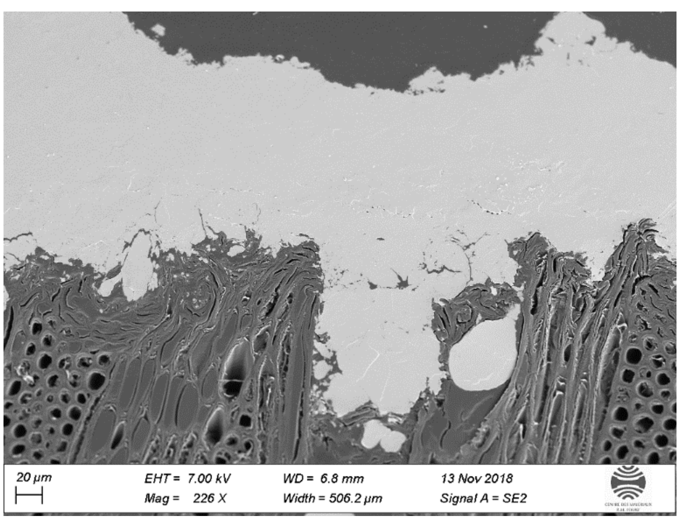

Fig 5: High pressure cold spray of tin onto sycamore transverse surface

Low pressure cold spray

LPCS technique extends the possibility to achieve a proper deposition onto sensitive substrates as wood and in any case where substrate erosion is a limiting factor for the coating build up. In fact, those equipments make possible to spray at lower pressure and high temperature, making sprayed particle softer and less erosive for the substrates.

In the case of aluminium powder, very high gas temperatures (more than 500°C) were used. Despite the downstream injection, the increase of the temperature caused frequent nozzle clogging and not many results were achieved. Nevertheless, some deposition was obtained onto all the surfaces, with low erosion and substantial particle deformation, but it was not possible to build up a proper coating with aluminium, as shown in the image below.

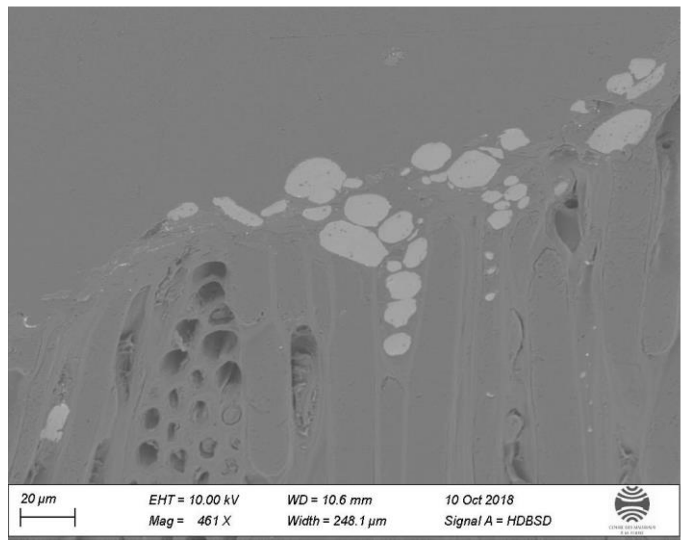

Fig 6: SEM cross section of LPCS of aluminum powder onto sycamore transverse surface.

Better results were obtained with tin powder. In this case, a proper deposition was obtained also on radial surfaces, while with HPCS only the transverse surface was successfully coated.

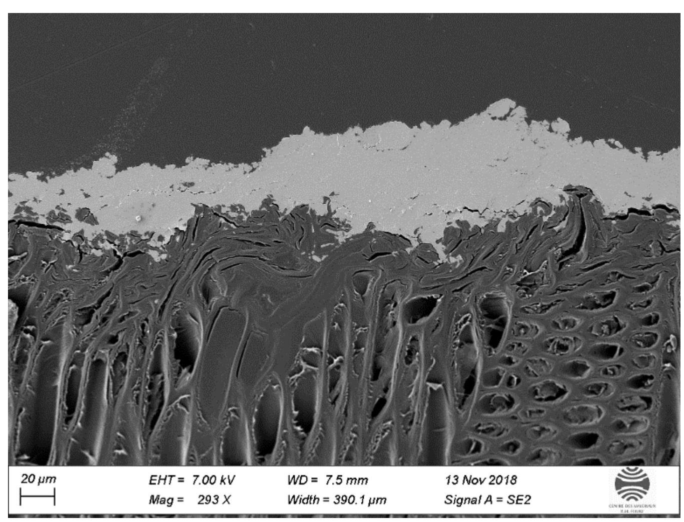

Fig 7: SEM cross section of LPCS of tin powder onto sycamore

transverse surface.

The coating on the transverse surface is shown in the SEM cross-section in Fig. 7. It is less dense and thick with respect to HPCS results, some cracks and porous zones can be seen.

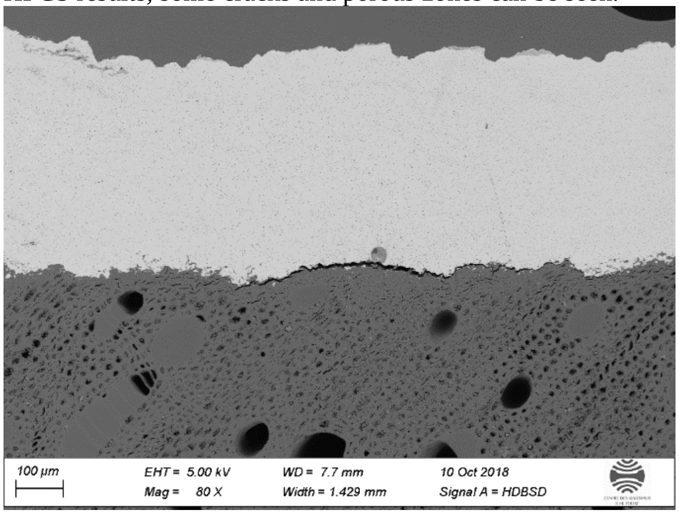

Fig 8: SEM cross section of LPCS of tin onto sycamore radial surface.

The coating on the radial (tangential) plane of the sycamore specimens is shown in the SEM cross-section in Fig. 8. The adhesion onto this surface seems to be less strong than onto the transverse one, since several cracks were found at the interface between wood and tin. This coating was successively used as a bond coat for the cold spray of copper powder. Unfortunately, only a thin non-continuous layer was found. Probably the copper powder used, characterized by a rather large mean size of more than 60 µm, was not an optimal choice for this application.

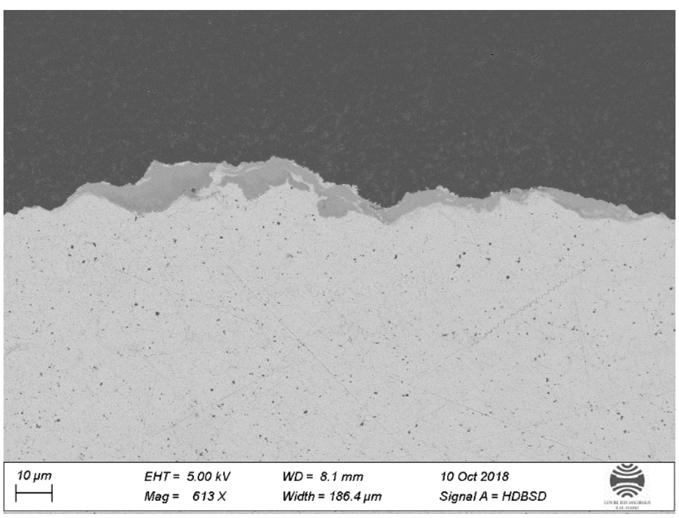

Fig 9: SEM cross section of LPCS of copper powder onto tin bond coat (Focus)

To obtain a copper coating, two powder mixtures were prepared. The first was composed by copper (80% vol) and a polymer [polyether ether ketone (PEEK)] (20% vol), the second one by copper (50% wgt) and zinc (50% wgt). These mixtures boosted the deposition possibility onto wood. Both deposits were found to be very thick and dense.

Since copper and PEEK powders have a huge difference in density, granulometry and volume, some regions in the coating, visible in Fig. 10, resulted to be richer in one of the two components. Moreover, a darker interface between the coating and the wood is visible, which is currently under investigation.

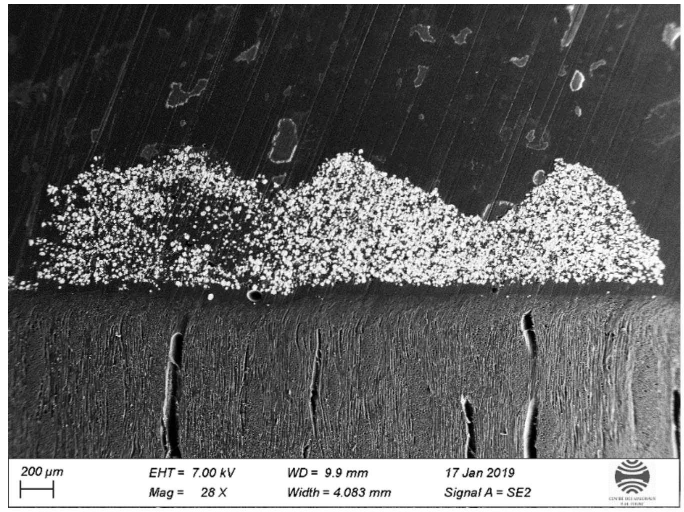

Fig. 10: low pressure cold spray copper-PEEK mixture coating onto tangential sycamore surface

The copper-zinc mixture was found to be the best combination for cold spraying onto wood. The differences in melting point and ductility of the two metals, allowed a very good deposition in terms of porosity and thickness, as can be seen in Fig. 11. Unfortunately, since the spraying temperature was rather high, the nozzle clogged, probably because of molten zinc.

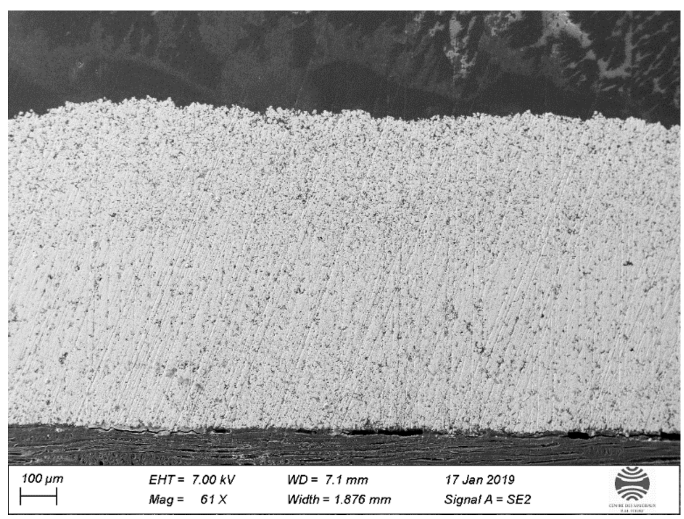

Fig. 11: *SEM cross section of LPCS of copper-zinc mixture powder onto sycamore radial surface.*

From a closer look under SEM at the interface between the metal coating and the wooden substrate, one can distinguish different behaviours of the wood structures. In the case of coatings onto the transverse surface, vessel were filled by undeformed particles that act as preferential bonding points for the particles impacting later, as visible in Fig. 12. When particles were bigger than the fiber diameters, impacts onto fibers resulted in the breakage of some and in the clogging of others promoting the starting of deposition process by following particles impacting onto them.

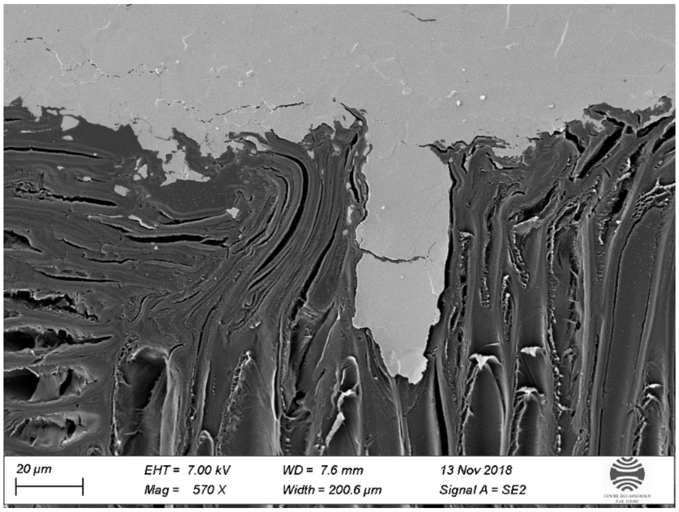

Fig 12: SEM cross section of LPCS of tin powder onto sycamore transverse surface (Focus on the interface)

In the case of coatings onto radial surfaces, particles impacted either onto the lateral walls of fibers and vessels or onto ray structures. The first two layers of fibers and vessels were probably highly damaged or completely destroyed by impinging particles. Then, fibers started to buckle, causing cell layers to cave in on themselves, as can be seen in Fig. 13. When fibers collapsed, their inner walls came into self-contact, causing an increase in stiffness. This mechanism then allowed the following particles to deform at impact and the beginning of coating building-up.

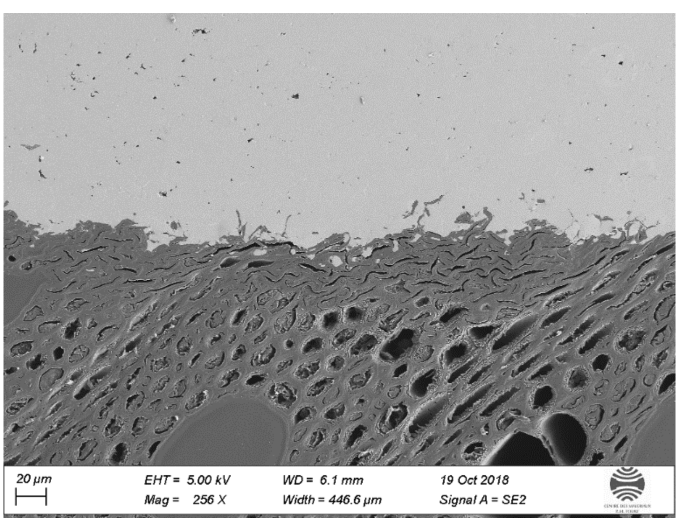

Fig 13:SEM cross section of LPCS of tin powder onto sycamore radial surface (Focus on interface)

Modelling of particle impact onto the wood surface

The first aim of numerical simulations of particle impact onto wooden surfaces is to understand and explain elementary phenomena controlling whether cold spray results in bare erosion of the substrate or in coating formation. In particular, metal particle interaction with local (at the particle scale) structures in the wood is crucial. For this purpose, some information that is needed to set up a correct modeling framework are: shape, velocity, temperature and material properties for particles and geometry and mechanical properties of wood structure at particle scale (10-100 µm). Computational fluid dynamic (CFD) results can be used as initial condition for such impact simulation. This development is ongoing (add some detail). SEM and microtomography could provide data for the representation of a simplified structure starting from real observations of the wood.

The modelling work of the cold spray deposition process has been well developed in recent years. The present study benefits from previous work at the laboratory [3]. Namely, an original modelling effort of the cold spray deposition process that was based on the development of a morphological stacking model and using the results of a finite element analysis of impact particle deformation. The model is intended to reflect reality as well as possible especially since the particles involved are numerous.

The size of the 3D modeling domain was identified as slightly larger than that of the cold sprayed particles. This corresponds to the so called meso-level structure of the wood, the level of fibers and vessels. At this scale, the material appears as a structure made up of objects of approximatively 10 µm (fibers) and 150 µm (vessels). As a first level of approximation, a simplified wood structure can be imagined as made up of extruded hexagonal cells, the fibers. In real wood, those cells are not hexagonal, and they show a variability of sizes and shapes.

The choice of the material model for the wood was more challenging, due to the novelty of the problem and the lack of literature investigating its material properties in conditions close to those of the cold spray process (micro scale and high speed impact).

As reported in [2], it can be assumed that cell walls consist of fiber-reinforced polymer laminates. Therefore, the mechanical behaviour of cell walls is similar to that of fiber-reinforced polymers. Typical behaviour for polymers is temperature dependent visco-elasticity.

When making numerical models to predict the collapse of a structure, a way of describing material failure is required. The damage model developed by Hashin [4] to describe failure in fiber-reinforced composites should be suitable to describe the failure modes and non-linearity of the cell walls (Fig. 14). Figure 14 introduces the four modes from O to A, where the undamaged elastic response of an element is shown, while A-C represents linear stiffness degradation. A is the point where damage is initiated for the current mode. The area under this graph is the fracture energy, GC, which is the energy dissipated due to failure in the current mode.

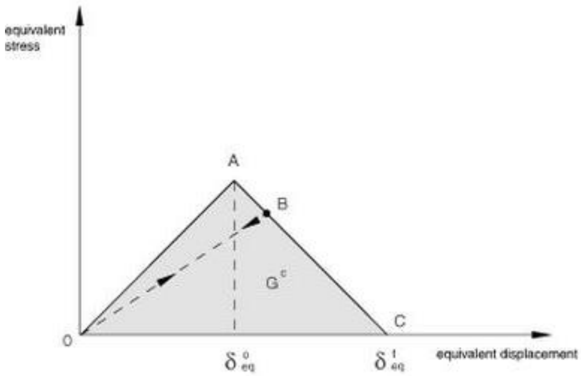

Fig. 14 Equivalent stress vs equivalent displacement, from [5]

This material behavior is expected to represent appropriately the mechanism of kinetic energy dissipation during the rupture of the fiber at impact. However, the tuning of the material parameters is a crucial task that should be fixed by means of experimental validation. One possible method to obtain this data is a nano-indentation test, which is currently under investigation.

The shell section (cell wall) was assigned to a regular honeycomb grid to create the cellular structure. The cell walls were modelled with two materials one describing the load bearing S2 layer (cellulose, hemicellulose and lignin lamina) and the other describing the compound middle lamella (lignin) acting as a binding matrix. S2 layer was modeled as a transversely isotropic lamina, lignin layer was then assumed to be isotropic. Properties are reported in Tables 3 & 4 below for the two layers.

Table 3: Mechanical properties of S2 layer from [2]

Mechanical properties of S2 material model	
E_1 (MPa)	35000
E_2 (MPa)	10000
ν	0.1 (Assumption)
G_{12} (MPa)	5000 (Assumption)
G_{13} (MPa)	5000 (Assumption)
G_{23} (MPa)	5000 (Assumption)
Density (kg/µm3)	$1.5*10^{-15}$

Table 4: Mechanical properties of S2 layer from [2]

Mechanical properties of Lignin material model	
E (MPa)	5200
ν	0.3

Material non-linearity is included by assigning the Hashin damage criterion to the S2 layer. The Hashin damage model consists of a damage initiation criteria and damage evolution description.

Required inputs for damage initiation in the Hashin damage are longitudinal and transverse tensile, compressive and shear strength, shown in Table 5.

Table 5: Inputs for damage initiation from [2]

Inputs for damage initiation (MPa)	
Longitudinal tensile strength	150
Longitudinal compressive strength	150
Transverse tensile strength	50
Transverse compressive strength	50
Longitudinal shear strength	150
Transverse shear strength	50

Damage evolution is described by a set of fracture energies, one for each damage mode. In this work one value was chosen to describe all the damage modes, shown in Table 6.

Table 6: Fracture energy value from [2]

Fracture energy	
G (N/m)	1000

A single copper particle with a velocity of 500 ms^{-1} is then added for the impact simulation. The material model chosen for the impacting particle is the Johnson-Cook model (Table 7). This is an empirical visco-plastic model which links the flow stress to the equivalent plastic strain, the plastic strain rate and the temperature. The terms of the equation respectively show hardening, strain rate hardening and thermal softening. This model is chosen because of its wide use in the literature and the few parameters it has. The equation is as follows:

$$\sigma = \left(A + B\varepsilon_p^n\right)\left(1 + C\ln\frac{\dot{\varepsilon_p}}{\dot{\varepsilon_0}}\right)\left(1 - T^m\right)$$

$$T = \frac{T - T_0}{T_{melt} - T_0}$$

Where:
σ is the yield stress (MPa)
ε_p the equivalent plastic strain (-)
$\dot{\varepsilon_p}$ the plastic strain rate (s^{-1})
$\dot{\varepsilon_0}$ reference plastic strain rate (s^{-1})
T_{melt} melting temperature of the material (°K)
T_0 reference temperature (°K)
A, B, C, n, m material parameters (MPa, MPa, -, -, -)

Table 7: Johnson Cook copper parameters from [6]

Johnson Cook Parameters	
$\dot{\varepsilon_0}$	1
T_{melt}	1356.16
T_0	283.15
A	90
B	292
C	0.025
n	0.31
m	1.09

The results of the simulation are still preliminary, because only one particle is involved and more representative parameters for the cell walls still have to be determined.

Nevertheless, this simulation approach is promising and some analogies with fibers behavior as experimentally observed are shown in Fig. 15.

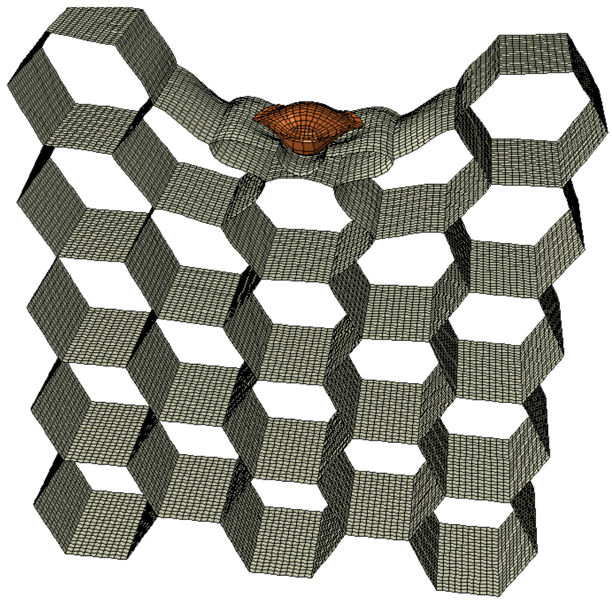

Fig 15: Impact simulation result of copper particle onto honeycomb reconstructed wooden microstructure.

Conclusions

The cold spray technology feasibility for innovative metal spraying onto wood was assessed in this work.
Nevertheless, cold spraying onto non-metallic and complex structures must be further investigated.
Particle adhesion and the coating build-up process onto wood seems to follow different behaviors compared to the classical metal onto metal case.
Thermo-sensitivity, pores and multiscale structures led to a new approach for the identification of intrinsic phenomena behind the deposition process onto wood.
Fiber rupture and buckling, filling of pores by impinging material and particle mechanical anchoring are all strictly connected. Even without a more quantitative approach in terms of velocity and temperature of the particles, deposition efficiency and adhesion strength, one can still draw some conclusions.
A gas increase in temperature and decrease in pressure were identified as the driving set of parameters to obtain deposition. In fact, heated and softer (maybe semi-molten) particles were effective in reducing erosion of the wooden substrate, although high temperatures (over 450°) could lead to surface combustion.
The transverse surface of wood showed better behavior in terms of erosion resistance, deposition efficiency and adhesion strength with respect to the other surfaces. This could be related to an interlocking and filling process of fibers and vessel that act as bonding points for subsequent particles.
Radial and tangential surfaces of wood, conversely, did not offer the same quality of bonding surface as the transverse ones, except for small area where rays were present. The first layers of the fibers were generally completely destroyed and embedded into the coating. Later, deeper fibers begin to buckle and, once they are compressed, provide an increased stiffness. Thus, the following particle impacts stop causing further erosion and instead begin to deform and build up a coating. The lack of interlocking points for particles impinging onto the radial surface caused lower adhesion strength of the deposit, leading to cracks and delamination.
Erosion and deposition phenomena show a strong dependence on the cold spray parameters, mainly stagnation pressure and temperature of the gas. To relate these parameters to impact condition of the particle is still a challenge. Velocity and temperature of the particle at the impact needs to be computed by means of a CFD model. This analysis will be extended to different nozzle shapes and dimensions as well as different injection points of the particles. In this way, cold spray equipment variables will also be investigated.
Finally, adhesion testing will provide quantitative data to assess the quality of the coating.

Acknowledgments

Special thanks to Ferdy Touwen and Klaas Rozema of Dycomet Europe for LPCS tests at Dycomet HQ.
Many thanks to my friend and colleague Sebastien Weiller, who helped me in dealing with HPCS equipment at MINESParisTech and with whom I share a sincere interest towards new perspectives in additive manufacturing.
The authors are grateful to DGA (French Army General Direction) for the financial support.

References

1. Wiedenhoeft, A. C., and Miller, R. B. (2005). “The structure and function of wood,”Chapter 2.in:Handbook of Wood Chemistry and Wood Composites, R. M.Rowell(ed.),CRC Press, Boca Raton, FL, USA, pp. 9–33 (15)
2. Trygve Stenrud Nilsen. Numerical modelling of Wood Microstructure, Master Thesis Norwegian University of Science and Technology. 2015.Smith, M. (2009).
3. Delloro, F., Jeandin, M., Jeulin, D. et al. J Therm Spray Tech (2017) 26: 1838. https://doi.org/10.1007/s11666-017-0624-8
4. Matzenmiller, A., J. Lubliner, and R.L. Taylor, A constitutive model for anisotropic damage in fiber-composites. Mechanics of Materials, 1995. 20(2): p. 125-152.
5. ABAQUS/Standard User's Manual, Version 6.9. Providence, RI: Simulia.P.H. Ralston and G.B. Hatch, U.S. Patent 3,803,038 [patent example]
6. R. Johnson, Gordon & H. Cook, William. (1985). Fracture characteristics of three metals subjected to various strains, strain rates, temperatures and pressure. Engineering Fracture Mechanics. 21. 31-48. 10.1016/0013-7944(85)90052-9.